Melting of anisotropically confined Coulomb balls

S. W. S. Apolinario* and F. M. Peeters†
Departement Fysica, Universiteit Antwerpen, Groenenborgerlaan 171, B-2020 Antwerpen, Belgium
(Received 14 April 2008; published 7 July 2008)

We found that an anisotropically confined Wigner crystal of Coulombic interacting particles exhibit inhomogeneous melting. The region of the system closest to the center of the cluster has a lower melting temperature than the extremum parts of the cluster. Moreover, the melting temperature of the cluster depends on the specific ordered three-dimensional (3D) state; i.e., it is larger when the cluster is in the multiple ring structure arrangement than when it has a nonsymmetric configuration.

DOI: 10.1103/PhysRevB.78.024202 PACS number(s): 64.60.−i, 47.57.−s

I. INTRODUCTION

Wigner crystallization[1] has been studied for decades in a variety of systems such as an electron gas trapped on top of liquid helium,[2] electrons trapped in quantum well structures,[3] strongly coupled rf dusty plasmas,[4] vortex clusters in an isotropic superfluid,[5] laser-cooled trapped ion systems,[6,7] and dusty plasmas.[8] Formation of ordered clusters with nested shells is expected to occur in expanding neutral plasmas.[9,10]

Charged classical particles isotropically confined by a three-dimensional (3D) external potential self-organize in concentric and almost equally spaced shells, which carry a specific number of particles. The number of shells depends on the total number of particles, and in general the number of shells increases with the number of particles. The ground-state (GS) configuration of systems of up to 12 particles consists of a single shell. These configurations in fact form three-dimensional regular polygons. From $N=13$ to 60, the arrangement of particles in the ground-state configuration form two shells except for the clusters with $N=58$ and 59 particles. For systems larger than 60 particles, ground-state configurations start to appear with three shells. (For a review about the static properties of 3D clusters, see Ref. 11.) The dynamics of small 3D clusters is expected to have different properties from that of large clusters due to finite size and symmetry effects which are stronger in small clusters.

In our previous work (Ref. 12), we investigated in detail the melting process of small isotropically confined 3D Wigner crystals of charged particles interacting through Coulomb or screened Coulomb potentials. We found that the GS configuration of systems with $N=6$, 12, 13, and 38 particles have large mechanical stability and are therefore identified as magic clusters. The common characteristic of magic clusters is that they are formed by one of the highly regular structures, i.e., an octahedron or icosahedron. For the system with $N=38$ particles, each fivefold coordinated particle sits in one of the corners of an icosahedron and is surrounded by sixfold coordinated particles.

The solid-liquid transition in nonmagic clusters was found to occur through two melting steps:[12] First, at low temperature the nonmagic cluster undergoes an intrashell melting; then, at higher temperature it undergoes a radial melting. Differently, pronounced resistance against intrashell diffusion is found in the magic cluster with $N=38$ particles, which gives the system the possibility to undergo an intermediate melting process, the so-called intershell melting.

The effect of the anisotropy of the confinement on the structural properties of 3D systems of equally charged particles was investigated in Ref. 13. The system was found to self-organize in three different general structures, i.e., multiple rings, degenerate multiple rings, and nonsymmetric structures, if the number of particles is small, typically $N\leq 25$ particles. For larger systems, i.e., $N\geq 50$, multiple ring structures were found in the external shell only if the anisotropy parameter was smaller than $\alpha\leq 0.2$, or in the internal shell for more isotropic confinements, roughly $\alpha\geq 0.4$. Our results on the structure of the GS configurations as a function of the anisotropy parameter were summarized in a phase diagram.

In this paper we investigate the dynamical properties of *anisotropically* confined Wigner crystals as an extension of our previous works[11–13] on isotropic Wigner balls. We investigate the homogeneity of the melting process and the effect of the different ordered states, i.e., degenerate multiple rings, multiple rings, and nonsymmetric structures, on the melting process of the system.

The paper is organized as follows: In Sec. III our model system is introduced, together with the methodology used to find stable configurations and the molecular-dynamics (MD) simulation approach. In Sec. III we investigate the melting process of small clusters, i.e., systems ranging from $N=10$ to 18 particles. In Sec. IV we investigate the melting process of larger clusters, i.e., systems with $N=30$ and 40 particles. Finally, in Sec. V we present our conclusions.

II. THEORETICAL MODEL

We study a 3D model system of N equally charged particles in an anisotropic confinement potential and interacting through a repulsive potential. The potential energy of the system is given by

$$E=\sum_{i=1}^{N}\frac{1}{2}m\omega_0^2(x_i^2+y_i^2+\alpha z_i^2)+\sum_{i>j}^{N}\frac{q^2}{\epsilon_0|\mathbf{r}_i-\mathbf{r}_j|}, \qquad (1)$$

where ϵ_0 and q are, respectively, the dielectric constant and the particle charge, $\mathbf{r}_i=(x_i,y_i,z_i)$ is the coordinate of the ith particle, N is the total number of particles, ω_0 is the confinement frequency, and α is the anisotropy parameter of the

confinement potential. We can write potential energy (1) in dimensionless form as

$$E = \sum_{i=1}^{N} (x_i^2 + y_i^2 + \alpha z_i^2) + \sum_{i>j}^{N} \frac{1}{|\mathbf{r}_i - \mathbf{r}_j|} \quad (2)$$

if we express the coordinate and energy in the following units: $r_0 = (q^2/\gamma\epsilon_0)^{1/3}$ and $E_0 = q^2/\epsilon_0 r_0$, where $\gamma = m\omega_0/2$. The temperature unit is given by $T_0 = E_0\kappa_B^{-1}$, where κ_B is the Boltzmann constant and $t_0 = \sqrt{2}/\omega_0$. All our numerical results will be given in dimensionless units.

The stable configuration is a local or global minimum of the potential energy, which is a function of only the number of charged particles N and the eccentricity α of the confinement potential. Our numerical method for obtaining the stable state configuration is based on the Monte Carlo simulation technique supplemented with the Newton method in order to increase the accuracy of the found energy value.[14] By starting from a large number of different random initial configurations, we believe that we were able to find all the possible stable (i.e., ground state and metastable) configurations. The configurational properties of anisotropically confined systems were discussed in detail in our previous paper.[13]

To study the dynamical properties of a small cluster at a specific temperature, first we use a variant of the velocity Verlet algorithm,[15] which rescales the velocity of the particles to bring the sample to a desired temperature. Second, we implement the MD simulation using the velocity Verlet algorithm.[15] A typical measurement done during this latter stage is the calculation of the averaged displacement of the particles from its equilibrium position.[16,17]

III. SMALL SYSTEMS

The GS configuration of a three-dimensional anisotropic Wigner crystal has three different ordered states,[13] i.e., multiple rings, degenerate multiple rings, and nonsymmetric configurations. The system with $N=18$ particles is one of the best representatives among the systems from $N=4$ up to 25 particles, since it has the three different structural phases as function of α.

The GS configuration of the cluster with $N=18$ particles and anisotropy parameter $\alpha=0.4$ is shown in Fig. 1. Such a GS configuration forms a multiple ring structure of arrangement $(1:(4\times)4:1)$; i.e., it has two particles situated in the extremities of the cluster along the z direction and a sequence of four rings with four particles each. Particles belonging to the same ring are represented by balls of the same color. Bounds between balls are drawn only for enhancing the visualization of the cluster.

The multiple ring structure can be thought of as a three-dimensional system formed by blocks of two-dimensional structures, i.e., the rings plus two isolated particles. In order to determine the melting temperature of the different block structures, we computed the radial averaged displacement [defined in Eq. (3)]. Such a quantity was computed for three different groups of particles, i.e., groups 1, 2, and 3, which are respectively represented by the symbols g_1, g_2, and g_3 in Fig. 1. Group g_1 comprises the two particles (represented by black balls) situated in the extremities of the cluster along the z direction. The third group, g_3, consists of the two most internal rings, i.e., the rings formed by the green and red balls (see Fig. 1). The second group, g_2, is formed by the two other rings, i.e., the rings formed by the violet and blue balls. It is clear from Fig. 1 that the cluster is symmetric with respect to the $z=0$ plane. All particles belonging to the same group have the same distance from the $z=0$ plane. As a result, the two different structures belonging to the same group have the same dynamical properties.

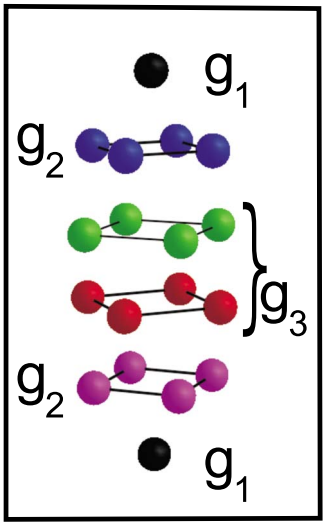

FIG. 1. (Color online) Ground-state configuration for the system with $N=18$ particles and anisotropy parameter $\alpha=0.4$. This configuration corresponds to a multiple ring structure with arrangement $(1:(4\times)4:1)$, i.e., four parallel rings with four particles each plus two isolated particles (black balls) situated in the extremities of the cluster along the z direction. The cluster is divided in three groups, i.e., groups 1 (g_1), 2 (g_2), and 3 (g_3).

The radial averaged displacement Δr is defined as follows:

$$\Delta r_\gamma^2 = 1/N_\gamma \sum_{i=1}^{N_\gamma} (\langle r_{\gamma i}^2 \rangle - \langle r_{\gamma i} \rangle^2)/a^2, \quad (3)$$

where γ can assume the values $\gamma=1,2$, and 3, which indicates, respectively, groups 1, 2, and 3. N_γ is the number of particles in group γ, $r_{\gamma i}$ is the modulus of the vector position of the ith particle of group γ, and a is the average distance between particles. The calculation of the radial averaged displacement as function of temperature allowed us to determine the different melting processes quantitatively. In order to characterize the melting temperature, we made use of a Lindemann-type criterion, which states that close to the melting process, the respective averaged displacement starts to deviate rapidly from its low-temperature linear dependence. We define the melting temperature as the temperature at which the radial averaged displacement changes its linear temperature dependence into a more rapid increase. Such a fact is also related to previous investigation in two-dimensional (2D) anisotropic Wigner crystals.[17,18]

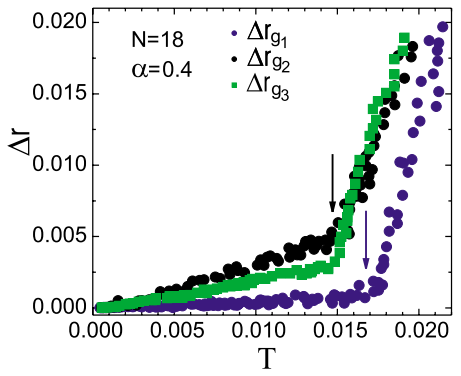

FIG. 2. (Color online) Radial averaged displacement computed for group 1 (Δr_{g_1}), group 2 (Δr_{g_2}), and group 3 (Δr_{g_2}) of the system with $N=18$ particles and anisotropy parameter $\alpha=0.4$.

Figure 2 shows the temperature dependence of the radial averaged displacement calculated for the different groups of particles belonging to the system with $N=18$ particles and anisotropy parameter $\alpha=0.4$. The radial averaged displacements Δr_{g_2} (black circles) and Δr_{g_3} (green squares) computed respectively for groups g_2 and g_3 increase rapidly at the same melting temperature, i.e., $T=0.015$ (Fig. 2, black arrow). The melting temperature for group g_1 is slightly larger, i.e., $T=0.017$ (Fig. 2, blue arrow).

The particle trajectory obtained during a time interval of 400 time steps in a MD simulation at a temperature of $T=0.016$ for the system with $N=18$ particles and anisotropy parameter $\alpha=0.4$ is shown in Fig. 3. It is apparent from Fig. 3 that the dynamical property of group g_1 is different from that of groups g_2 and g_3. While the two particles belonging to group g_1 (Fig. 3, black balls) remain oscillating around their equilibrium position, particles of groups g_2 and g_3 do not have a localized trajectory around their equilibrium positions. Rather, we can see that at the temperature of $T=0.016$ particles belonging to one ring are already able to jump to a position in the neighboring ring.

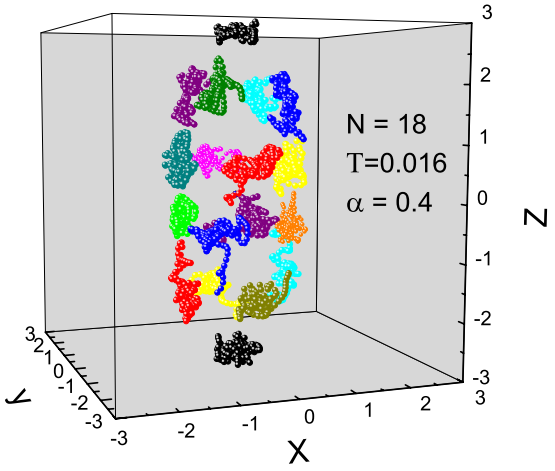

FIG. 3. (Color online) Particle trajectories obtained during a time interval of 400 time steps for a system with $N=18$ particles and anisotropy parameter $\alpha=0.4$ at a temperature of $T=0.016$. Different colors were used to distinguish between trajectories of neighboring particles.

The latter results, i.e., Figs. 2 and 3, showed that the melting process for the system with $N=18$ particles and anisotropy confinement $\alpha=0.4$ is inhomogeneous. In other words, the melting process does not involve all particles; i.e., the center of the cluster (regions g_2 and g_3) melts first before the extremities of the cluster, i.e., group g_1, with increasing temperature. Such a picture is different from the one we found for small isotropic systems.[12] In the latter, the first melting process is an intrashell melting, i.e., a low-temperature melting process involving all particles of the cluster.

In this paper we want to characterize the melting process of anisotropic systems. Toward this objective, we will calculate the z averaged displacement. Such a quantity is defined analogously as done for the radial averaged displacement [Eq. (3)] except that r is replaced by z.

Moreover, for any given system we will define two groups of particles: the external group g_{ext}, i.e., the group formed by the set of two particles most distant from the center of the cluster, i.e., with the largest modulus of the z coordinate of the position vector; and the internal group g_{in}. For the case of the GS configuration shown in Fig. 2, the external group g_{ext} would correspond to group g_1, while the internal group g_{in} would correspond to the sum of groups g_2 and g_3. The corresponding melting temperatures for the z averaged displacement in the internal and external groups will be indicated by T_{ext} and T_{in}, respectively.

The z averaged displacement will be computed for the internal and external groups. The melting process is considered inhomogeneous if the following condition is satisfied: the value of the critical temperature of the external group T_{ext} is larger than T_{in} and T_{ext} is larger than T_m, where T_m is the melting temperature of the system which is given by the calculation of the radial averaged displacement.

Figures 4(a)–4(c) show the temperature dependence of the z averaged displacement for the internal groups, Δz_{in} (red squares), and external groups, Δz_{ext} (black triangles), and the radial averaged displacement Δr (blue circles) for the whole system with $N=18$ particles and anisotropy parameters equal, respectively, to $\alpha=0.2$, 0.5, and 1.0. The melting temperature for the isotropic system ($\alpha=1$) is equal to $T_m=0.051$ [Fig. 4(c), blue arrow]. We can see that the z averaged displacements calculated in the internal and external groups increase very rapidly immediately when $T\neq 0$ [see blue squares and black triangles in Fig. 4(c)]. The latter result shows that the melting process is homogeneous. The very rapid increase in the z averaged displacement near $T\approx 0$ is due to the intrashell melting process which occurs at very low temperatures.[12]

From Fig. 4(a) we can see that the radial averaged displacement Δr and the z averaged displacement calculated for the internal group, Δz_{in}, increase rapidly at the same temperature $T=0.016$ [see Fig. 4(a), black arrow]. The critical temperature for the external group has a larger value, i.e., $T=0.038$ [see Fig. 4(a), red arrow]. Such a situation indicates that for an anisotropy parameter of $\alpha=0.2$, the melting process of the system with $N=18$ particles is inhomogeneous. Analogously, from Fig. 4(b) we can see that the melting process for an anisotropy parameter of $\alpha=0.5$ is also inhomogeneous. For this latter case, the melting temperatures of the system, $T_m=0.0023$ [Fig. 4(b), blue arrow], and of the inter-

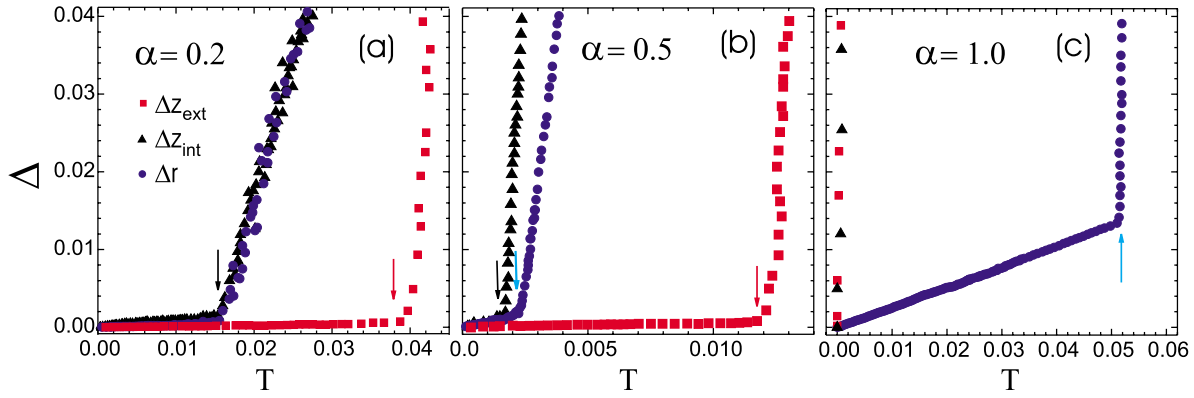

FIG. 4. (Color online) Temperature dependence of the z averaged displacements computed for the external and internal groups, i.e., Δz_{ext} (red squares) and Δz_{in} (black triangles), respectively, and the radial averaged displacement Δr (blue circles). (a), (b), and (c) correspond to the system with $N=18$ particles and anisotropy parameter equal to $\alpha=0.2$, 0.5, and 1.0, respectively.

nal group, $T_{\text{in}}=0.0018$ [Fig. 4(b), black arrow], are both smaller than the critical temperature of the external group, $T_{\text{ext}}=0.012$ [Fig. 4(b), red arrow]; i.e., the melting process does not involve all particles.

Figure 5 shows the melting temperature T_m (blue circles) and the critical temperatures for the internal groups, T_{in} (black triangles), and external groups, T_{ext} (red squares), for different system sizes as function of the anisotropy parameter. In each figure the region of α corresponding to nonsymmetric configurations are left blank, while the regions of α corresponding to degenerate multiple rings or multiple ring structures are colored. Moreover, the symmetric arrangement of particles, i.e., multiple rings and degenerate multiple rings, are indicated for each system.

The critical temperatures for the system with $N=18$ particles and different values of the anisotropy parameter are shown in Fig. 5(f). We can see from Fig. 5(f) that for $\alpha > 0.7$ the melting process becomes homogeneous, i.e., $T_m > T_{\text{ext}}$, while that for $\alpha < 0.7$ the melting process becomes inhomogeneous, i.e., $T_m < T_{\text{ext}}$. Moreover, Fig. 5(f) also reveals that the decrease in the melting temperature is not monotonic with decrease in the value of α. In fact, we notice [see red arrows in Fig. 5(f)] that for values of the anisotropy parameter where the GS configuration corresponds to a symmetric arrangement, i.e., multiple rings or degenerate multiple rings, the melting temperature T_m of the system is enhanced. For example, for the anisotropy parameter $\alpha=0.4$, whose GS configuration corresponds to a multiple ring structure of arrangement $(1:(4\times)4:1)$, the melting temperature is $T_m=0.016$, while that for a nonsymmetric structure at the anisotropy parameters of $\alpha=0.3$ and 0.5 the melting temperature are, respectively, $T_m=0.003$ and 0.0035. Nevertheless, we can see that the melting temperature of the system initially decreases with decreasing anisotropy parameter. For instance, for $\alpha=1.0$ the melting temperature is $T_m=0.051$ and its value decreases to $T_m=0.048$, 0.040, 0.011, and 0.006

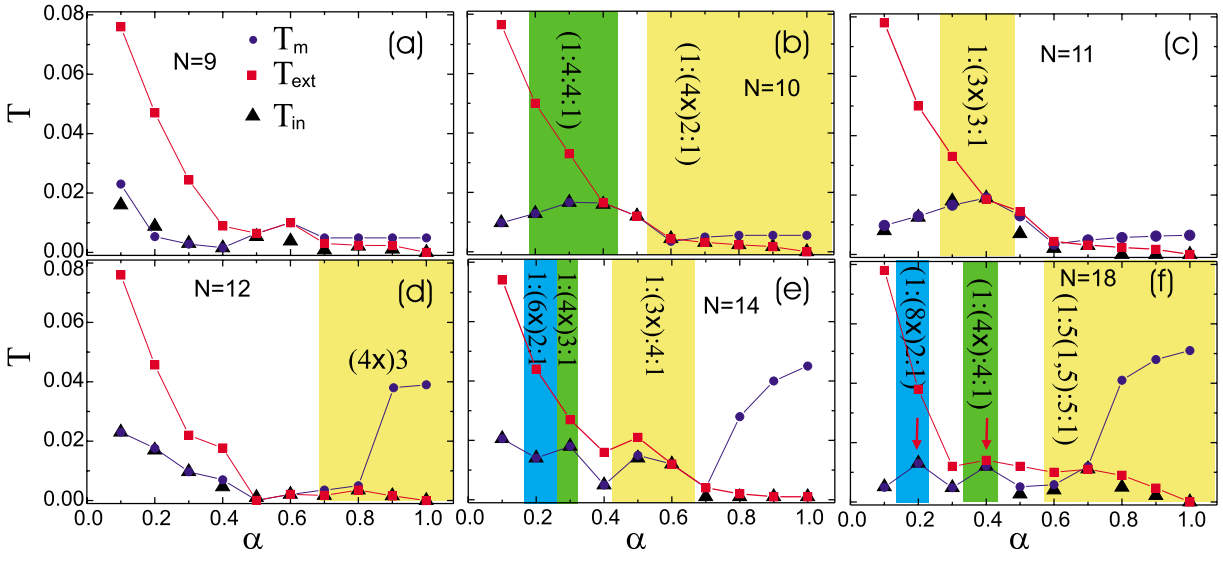

FIG. 5. (Color online) The critical temperature of the system T_m (blue circles), the critical temperature of the external (T_{ext}) and internal (T_{in}) groups of particles are shown for systems with different number of particles, N, as a function of the anisotropy parameter α. In each figure the region of α corresponding to nonsymmetric configurations are left blank. The regions of α corresponding to degenerate multiple rings or multiple ring structures are colored as blue, green, and yellow; the symmetric arrangements are indicated.

for α=0.9, 0.8, 0.7, and 0.6, respectively. Isotropic systems have large melting temperature due to the large value of the potential barrier between shells. If the temperature of the system is small, particles will remain trapped to one of the shells and will not have enough kinetic energy to overcome the potential barrier between shells. However, as the anisotropy parameter decreases, the cluster gradually obtains a more prolate shape. In a prolate cluster, the distance between particles belonging to the different elliptic shells is smaller than the ones in a spherical cluster. As a result, prolate clusters have lower barrier potentials between shells than spherical clusters. This is the reason that the melting temperature of slightly anisotropic systems is reduced when decreasing the value of the anisotropy parameter.

The GS configuration for the system with N=9 particles does not have high-symmetry arrangements. We calculated the critical temperature of this system for different values of the anisotropy parameter [see Fig. 5(a)]. One notices that initially the melting temperature of the system T_m decreases as the anisotropy parameter decreases. Moreover, the system with N=9 particles also presents inhomogeneous melting for very anisotropic confinements, i.e., $\alpha < 0.5$. For example, for α=0.1 the melting temperature of the system is T_m=0.023, while the critical temperature of the external group is much larger, i.e., T_{ext}=0.079.

The systems with N=10, 11, and 14 particles have regions of the anisotropy parameter α where the GS configurations correspond to a high-symmetry arrangement. Those regions are indicated by the colored areas in Figs. 5(b), 5(c), and 5(e), respectively. In all cases we can find an increase in the melting temperature when the system is in the multiple ring or degenerate multiple ring configuration. Moreover, for very anisotropic confinements, the critical temperature of the external group T_{ext} (red squares) is substantially larger than the melting temperature of the system T_m (blue circles). For example, for the system with N=10, 11, 12, and 14 and α=0.1 [see, respectively, Figs. 5(b)–5(e)], the melting temperatures are much lower, i.e., T_m=0.010, 0.0094, 0.022, and 0.02, respectively, than the critical temperature of the external groups, i.e., T_{ext}=0.079, 0.078, 0.079, and 0.075, respectively.

IV. LARGE SYSTEMS: N=30 AND 40

The melting process of small isotropically confined Wigner crystals consists of two steps as the temperature of the system increases:[12] First, at low temperature, intershell melting takes place; and when temperature is further increased, finally radical melting occurs. The increase in the number of particles leads to the formation and growth of a body-centered cubic particle arrangement in the internal region of the cluster. As a result, the two melting steps typically found in small clusters gives way to a melting process ruled by the dynamics found in the bulk of the cluster.[19]

In Sec. III we showed that inhomogeneous melting is typical for highly anisotropic clusters, i.e., roughly for anisotropy parameter $\alpha \leq 0.5$. In this section we investigate how the inhomogeneous melting process responds to an increase in the cluster size. As an example, we consider systems with N=30 and 40 particles.

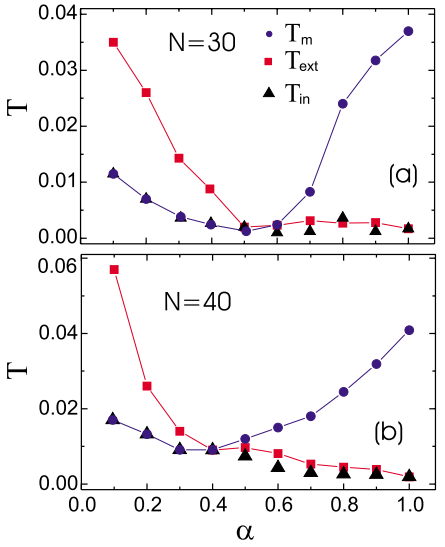

FIG. 6. (Color online) (a) and (b) display the critical melting temperatures as function of the anisotropy parameter for systems with N=30 and 40 particles, respectively.

The distinct critical temperatures for the system with N=30 particles and anisotropy parameter varying from α=0.1 to 1.0 in steps of $\Delta\alpha$=0.1 are shown in Fig. 6(a). From Fig. 6(a) we can clearly see that the melting process is inhomogeneous (homogeneous) when $\alpha < 0.5$ ($\alpha > 0.5$). Analogously, we find the same picture for the system with N=40 particles [see Fig. 6(b)]. In the latter case, the critical value of the anisotropy parameter, i.e., the value of α which separates the inhomogeneous from the homogeneous melting regimes, is equal to α=0.4. We found that this is a general trend, namely, the critical α value decreases with increasing N.

V. CONCLUSIONS

Using MD simulation, we investigated the melting processes of a finite-size 3D system of equally charged particles confined by an external anisotropic confinement potential. We assumed that the particles interact via a Coulombic interparticle interaction potential. Our theoretical model is applicable to systems such as dusty plasmas and colloids. It is expected that the found physical behavior is qualitatively the same for other isotropic interaction potentials as, e.g., a screened Coulomb potential.

We found that the melting of the system becomes inhomogeneous, i.e., the melting process is not uniform throughout the cluster, as the anisotropy parameter decreases. The region of the system closest to the center of the cluster has lower melting temperature than the extremum parts of the cluster. Additionally, the melting temperature of the cluster depends on the specific ordered state; i.e., it is larger when the cluster is in the multiple ring or degenerate multiple ring configuration. Moreover, inhomogeneous melting was verified to happen both for small and large systems.

ACKNOWLEDGMENT

This work was supported by the Flemish Science Foundation (FWO-Vl).

*sergio.apolinario@ua.ac.be
†francois.peeters@ua.ac.be

[1] E. P. Wigner, Phys. Rev. **46**, 1002 (1934).
[2] C. C. Grimes and G. Adams, Phys. Rev. Lett. **42**, 795 (1979).
[3] E. Y. Andrei, G. Deville, D. C. Glattli, F. I. B. Williams, E. Paris, and B. Etienne, Phys. Rev. Lett. **60**, 2765 (1988).
[4] J. H. Chu and I. Lin, Phys. Rev. Lett. **72**, 4009 (1994).
[5] Y. Kondo, J. S. Korhonen, M. Krusius, V. V. Dmitriev, E. V. Thuneberg, and G. E. Volovik, Phys. Rev. Lett. **68**, 3331 (1992).
[6] W. M. Itano, J. J. Bollinger, J. N. Tan, B. Jelenković, X.-P. Huang, and D. J. Wineland, Science **279**, 686 (1998).
[7] L. Hornekær, N. Kjærgaard, A. M. Thommesen, and M. Drewsen, Phys. Rev. Lett. **86**, 1994 (2001).
[8] O. Arp, D. Block, A. Piel, and A. Melzer, Phys. Rev. Lett. **93**, 165004 (2004).
[9] T. Pohl, T. Pattard, and J. M. Rost, Phys. Rev. Lett. **92**, 155003 (2004).
[10] T. Killian, Nature (London) **429**, 815 (2004).
[11] S. W. S. Apolinario, B. Partoens, and F. M. Peeters, New J. Phys. **9**, 283 (2007).
[12] S. W. S. Apolinario and F. M. Peeters, Phys. Rev. E **76**, 031107 (2007).
[13] S. W. S. Apolinario, B. Partoens, and F. M. Peeters, Phys. Rev. B **77**, 035321 (2008).
[14] V. A. Schweigert and F. M. Peeters, Phys. Rev. B **51**, 7700 (1995).
[15] L. Verlet, Phys. Rev. **159**, 98 (1967); **165**, 201 (1968).
[16] V. M. Bedanov and F. M. Peeters, Phys. Rev. B **49**, 2667 (1994).
[17] S. W. S. Apolinario, B. Partoens, and F. M. Peeters, Phys. Rev. E **72**, 046122 (2005).
[18] S. W. S. Apolinario, B. Partoens, and F. M. Peeters, Phys. Rev. E **74**, 031107 (2006).
[19] J. P. Schiffer, Phys. Rev. Lett. **88**, 205003 (2002).